Towards quantitative SERS detection of hydrogen cyanide at ppb level for human breath analysis

Lauridsen, Rikke Kragh; Rindzevicius, Tomas; Molin, Søren; Johansen, Helle Krogh; Berg, Rolf W.; Alstrøm, Tommy Sonne; Almdal, Kristoffer; Larsen, Flemming; Schmidt, Michael Stenbæk; Boisen, Anja

Published in:
Sensing and Bio-Sensing Research

Link to article, DOI:
10.1016/j.sbsr.2015.07.002

Publication date:
2015

Document Version
Publisher's PDF, also known as Version of record

Sensing and Bio-Sensing Research 5 (2015) 84–89

Contents lists available at ScienceDirect

Sensing and Bio-Sensing Research

journal homepage: www.elsevier.com/locate/sbsr

Towards quantitative SERS detection of hydrogen cyanide at ppb level for human breath analysis

Rikke Kragh Lauridsen [a,*], Tomas Rindzevicius [a], Søren Molin [b], Helle Krogh Johansen [b,c], Rolf Willestofte Berg [d], Tommy Sonne Alstrøm [e], Kristoffer Almdal [a], Flemming Larsen [a], Michael Stenbæk Schmidt [a], Anja Boisen [a]

[a] DTU Nanotech, Technical University of Denmark, Department of Micro- and Nanotechnology, Ørsteds Plads, Building 345 East, DK-2800 Lyngby, Denmark
[b] DTU Biosustain, Technical University of Denmark, Novo Nordisk Foundation Center for Biosustainability, Kogle Allé 6, DK-2970 Hørsholm, Denmark
[c] Department of Clinical Microbiology 9301, Rigshospitalet, Juliane Maries Vej 22, DK-2100 København Ø, Denmark
[d] DTU Chemistry, Technical University of Denmark, Department of Chemistry, Kemitorvet, Building 206, DK-2800 Lyngby, Denmark
[e] DTU Compute, Technical University of Denmark, Department of Applied Mathematics and Computer Science, Richard Petersens Plads, Building 321, DK-2800 Lyngby, Denmark

ARTICLE INFO

Article history:
Received 25 March 2015
Revised 23 June 2015
Accepted 1 July 2015

Keywords:
Surface-Enhanced Raman Spectroscopy
Hydrogen cyanide
Pseudomonas aeruginosa
Cystic fibrosis
Breath analysis

ABSTRACT

Lung infections with *Pseudomonas aeruginosa* (PA) is the most common cause of morbidity and mortality in cystic fibrosis (CF) patients. Due to its ready adaptation to the dehydrated mucosa of CF airways, PA infections tend to become chronic, eventually killing the patient. Hydrogen cyanide (HCN) at ppb level has been reported to be a PA biomarker. For early PA detection in CF children not yet chronically lung infected a non-invasive Surface-Enhanced Raman Spectroscopy (SERS)-based breath nanosensor is being developed. The triple bond between C and N in cyanide, with its characteristic band at ~2133 cm^{-1}, is an excellent case for the SERS-based detection due to the infrequent occurrence of triple bonds in nature. For demonstration of direct HCN detection in the gas phase, a gold-coated silicon nanopillar substrate was exposed to 5 ppm HCN in N_2. Results showed that HCN adsorbed on the SERS substrate can be consistently detected under different experimental conditions and up to 9 days after exposure. For detection of lower cyanide concentrations serial dilution experiments using potassium cyanide (KCN) demonstrated cyanide quantification down to 1 μM in solution (corresponding to 18 ppb). Lower KCN concentrations of 10 and 100 nM (corresponding to 0.18 and 1.8 ppb) produced SERS intensities that were relatively similar to the reference signal. Since HCN concentration in the breath of PA colonized CF children is reported to be ~13.5 ppb, the detection of cyanide is within the required range.

1. Introduction

Cystic fibrosis (CF) patients have a salt imbalance of the secretory cells leading to excessive, salty sweating and swelling of the pancreatic duct, accompanied by an insufficient uptake of proteins and lipids. The most commonly known symptom is swelling of the bronchial wall due to vastly dehydrated and thickened mucus and bacterial infections, leading to coughing and loss of breath. Bacteria often infect the sinuses, and it has been shown that they adapt to the lower airways in the sinuses and drop into the lungs e.g. during sleep or viral infections [12,15]. The bacterium most commonly associated with morbidity and mortality in CF patients is *Pseudomonas aeruginosa* (PA) which is harmless to healthy individuals but well-adapted to the oxygen depleted environment in the upper airways [1]. The intermittent PA lung colonization often becomes chronic, which is why early detection and eradication is essential [19].

P. aeruginosa emits the poisonous gas hydrogen cyanide (HCN) to outmatch competitive microorganisms, and HCN has been suggested as a potential PA biomarker [4,9,16]. Selected ion flow tube mass spectrometry (SIFT-MS) and other MS based principles are among the most frequently applied techniques for human breath analysis, detecting HCN levels between 0 and 81 ppb [2,7,9–11,21,29]. Because HCN is also formed in the oral cavity of adults it has been suggested to only use nose exhaled breath for analysis in adult CF patients. A "cut-off" value of 10 ppb has been suggested as "elevated", indicative of a PA infection [10]. In the breath of CF children with a PA airway colonization HCN has been reported to lie between 8.1 and 16.5 ppb, with a median value of 13.5 ppb [9]. For a definition of PA colonization versus chronic infection please refer to [14].

* Corresponding author.
E-mail address: rkla@nanotech.dtu.dk (R.K. Lauridsen).

http://dx.doi.org/10.1016/j.sbsr.2015.07.002
2214-1804/

For mouse model systems secondary electron spray ionization mass spectrometry (SESI-MS) has been used for *in vivo* breath diagnosis of lung infection models [30,31]. The authors point out that *in vitro* studies cannot be expected to mimic *in vivo* results because only between 25% and 27% of the *in vitro* and *in vivo* PA peaks were shared. For analysis of sputum and broncho-alveolar lavage (BAL) samples various electrochemical probes have been used to measure cyanide content at micromolar level [3,11,22,27]. The techniques for breath analysis are either, expensive, inflexible, time consuming or they demand a high level of operator skills [5]. Therefore, there is a need for a fast, inexpensive and sensitive sensor for the detection of *P. aeruginosa* in the breath of children with cystic fibrosis.

Raman scattering spectroscopy is a widely used fingerprinting method for small molecules. However since it is not a very sensitive method, millimolar concentration seems to be the limit of detection [6]. Surface-Enhanced Raman Spectroscopy (SERS) using gold nanoparticles in a sol–gel has been used to detect ppb level cyanide in waste water [20], and in 2011 Senapati et al. reported to have detected cyanide in the ppt range by the use of Au SERS aggregation [26]. In the presence of noble metals, cyanide can be detected due to its high affinity towards metals. These approaches demand cyanide to be in solution for SERS detection and there is much sample preparation. We propose a fast and cheap technique based on the SERS substrate developed by Schmidt et al. [24] that can be used both in solution and for the direct detection of cyanide in gas phase as a precursor for PA breath detection. The substrate consists of gold coated silicon nanopillars which can be brought to lean against each other, forming so-called "hot spot" regions with considerate plasmonic effect for Raman signal enhancement to take place. It is well-known that Raman is a quantitative method [25] and in some cases it is also possible to perform quantitative SERS, although it has yet to be demonstrated to a wider extent [8].

Hydrogen cyanide is a potential PA biomarker. If a point-of-care device could detect HCN in the breath of young CF patients with a pulmonary PA colonization, the need for invasive techniques and repeated anesthesia for obtaining broncho-alveolar lavage to diagnose PA would be minimized. To make a simple model system for the presence of HCN in breath, a gas setup with an open flow cell connected to a tank of 5 ppm HCN(g) in N_2 was used. The SERS substrate was placed inside the flow cell and exposed to the gas for 30 s. To vary the amount of HCN molecules exposing the substrate, the pressure through the open system was changed among samples.

In the present paper SERS measurements on 5 ppm HCN gas and on serial dilutions of potassium cyanide (KCN) in the region from 10 nM to 1 mM are presented. A KCN concentration range of 100 nM to 1 μM is the region of relevance, corresponding to ppb gas levels. The aim of the project is to detect PA colonization in the patients' breath at an earlier stage than allowed by today's conventional methods.

2. Experimental

2.1. SERS substrate fabrication and measurement procedure

Nanopillars were etched into a Si wafer in an Advanced Silicon Etcher, applying alternate portions of SF_6 and O_2 plasma (dry etch), followed by an O_2 cleaning step. The resulting nanopillars are 400 nm in height, 50 nm in width, and with a density of approximately 18 pillars/μm^2. A 225 nm thin Au layer was then deposited onto the silicon nanopillars, producing freely standing Au-capped Si nanopillar structures (Fig. 1(a)). The wafer was diced into 6 × 6 mm^2 squares using a diamond cutter and the substrates were used within 1–2 days after Au deposition.

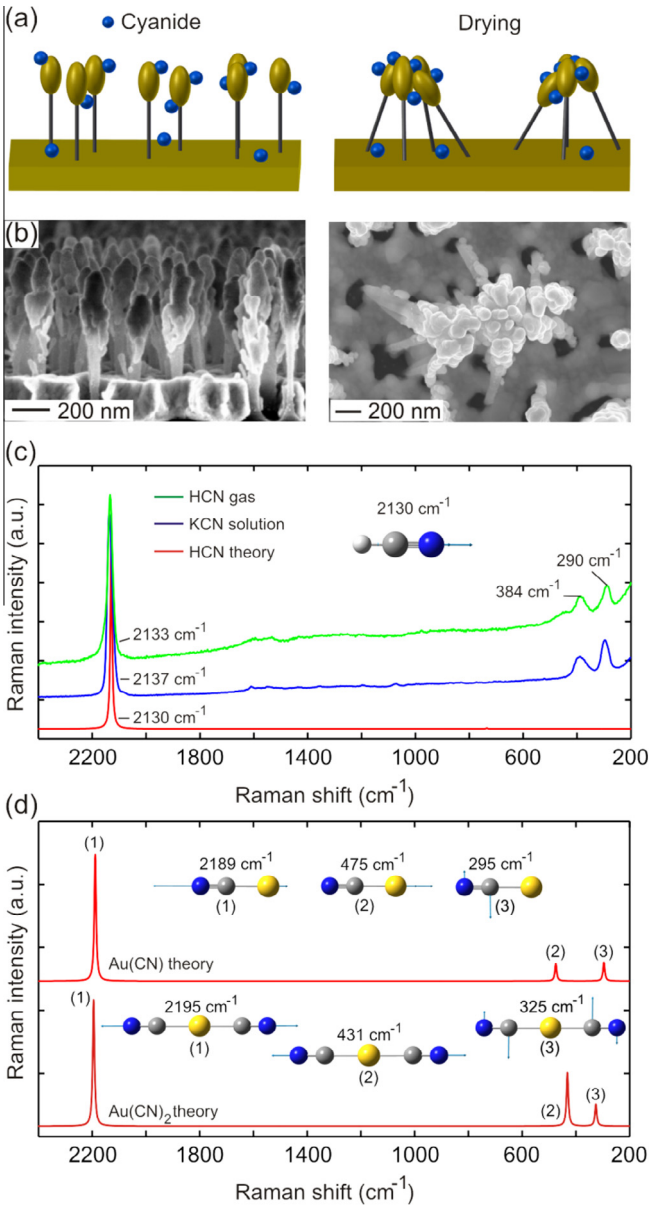

Fig. 1. (a) Illustration of the leaning of nanopillars. When immersed in liquid and subsequently dried, capillary forces make the pillars lean against each other, creating SERS "hot spots" for enhancement of the Raman signal. (b) SEM images of the Au-coated Si SERS substrate, before and after leaning (Courtesy of Kaiyu Wu). (c) SERS spectra of HCN(g) and KCN(aq) on the Au SERS substrate and theoretical Raman spectrum of HCN. (d) Theoretical Au(CN) and $Au(CN)_2^-$ Raman spectra.

The measurements were conducted in a DXR dispersive SmartRaman spectrometer with thermoelectric CCD cooling, an optical microscope and a 780 nm excitation laser from Thermo Fisher Scientific. An optical microscope was coupled to a single grating spectrometer with 5 cm^{-1} FWHM spectral resolution and ±2 wavenumber accuracy. Two times 5 s scan time at a laser power of 5.0 mW was applied through a 25 μm slit using a 10× magnification lens. Raman wavenumber shifts were collected in the region 100–3400 cm^{-1}. In each experiment all SERS substrates were prepared from the same wafer. In order to avoid cross contamination of the sensitive substrates, samples with different KCN concentrations were left to dry separately and kept in small Petri dishes for transport and storage. One substrate was prepared for each concentration and 10 points were measured for each SERS substrate. In the HCN gas experiments each SERS substrate was

exposed to different HCN gas flow conditions. The SERS signal was then recorded from 10 random points from each SERS substrate. Therefore, the data points in Figs. 2(b), 4(b) and 5(b) show the SERS signal intensity variations (cyanide peaks) measured for a given experimental condition from 10 different measurement points from a single SERS chip. Reference SERS signals were recorded using water droplets prior to KCN or HCN exposures. In all cases a weak Raman band close to 2120 cm^{-1} that is likely due to carbonaceous species on the Au surface is observed [17].

2.2. Gas setup

Five ppm HCN(g) in N_2 from the supplier AGA (Linde AG, Pullach, Germany) was used for cyanide gas exposure. Four ppm was the lowest stabile concentration the supplier could guarantee. The setup consists of an open flow cell connected with a pressure controlled gas inlet, see insert in Fig. 2(a). The meter to the right indicates the amount of gas left in the tank while the barometer to the left shows the pressure within the system. The large regulator is for gas flow regulation, and the small one is for opening and closing the gas flow. Thus, when the gas flow is increased, the pressure inside the system rises which can be read on the barometer.

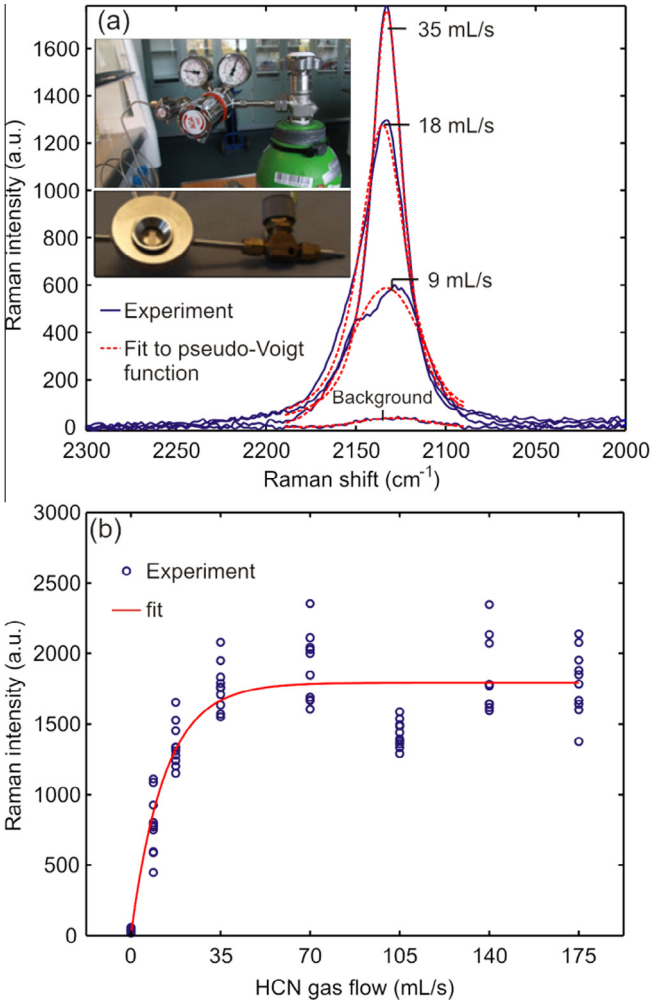

Fig. 2. a (insertion) Setup for 5 ppm HCN gas exposure, including the flow cell in the insertion below. (a) Representative Raman spectra of the pre-leaned SERS substrates exposed to 30 s 5 ppm HCN(g) at 35; 18; and 9 mL/s flow, 30 min. after exposure. The C≡N stretching band at 2134 cm^{-1} is clear and distinct, increasing with increasing flow. (b) 2134 cm^{-1} peak intensity at various gas flows. Above 35 mL/s the signal saturates, corresponding to a gas concentration of 5 ppm.

Via a simple setup using an upturned measuring cylinder in a water bath it was shown that 0.2 bar in the system corresponds to 35 mL/s gas flow. The gas flow is expected to correlate with HCN(g) concentration at low flow-rate. After the regulator, the gas passes through a steel tube to the flow cell placed in the fume hood (bottom insert in Fig. 2(a)). The SERS substrate was placed on a platform inside the flow cell. Prior to gas exposure the SERS substrate was cleaned by 3 min immersion in very pure ethanol (Absolute grade, CHROMASOLV®, Sigma–Aldrich) followed by 3 min rinsing in water (Molecular Biology Reagent grade, Sigma–Aldrich) and left to dry on a clean tissue. The drying caused the nanopillars to lean against each other, see Fig. 1(a) and (b). The cell was purged with the relevant flow for 2 min before the SERS substrate was placed in the flow cell and exposed to the gas for 30 s. In all cases the flow was changed in a random order not to confound the results by sequence of exposure. The gas setup was used for verification of gas detection on the SERS substrate.

2.3. KCN solutions

Aqueous cyanide solutions of potassium cyanide (KCN) were prepared as a model system for precise control of the concentration of cyanide in solution. According to Henry's law either the temperature should be kept low or pH should be high in order to keep cyanide in the solution, preventing it from evaporating as HCN(g) [18]. It would not be feasible to maintain a low temperature, and the approach with pH adjustment was therefore adopted. KCN solutions from 10 nM to 1 mM were prepared and their pH was adjusted to 11 by the addition of NaOH. The SERS substrates were cleaned by 3 min immersion into ethanol (Absolute grade, CHROMASOLV®, Sigma–Aldrich), followed by 3 min in water (Molecular Biology Reagent grade, Sigma–Aldrich). From there they were immersed directly into the KCN solution for 3 min before drying on a clean tissue, making the nanopillars lean against each other, ready for measurements. Due to strong gold-cyanide bonding all cyanide on the substrate is expected to be captured on the nanopillars while the water evaporates. Water with added NaOH to pH 11 was used as reference.

2.4. Data analysis

Theoretical Raman spectra in vacuum were calculated using Gaussian 09W, methods DFT/B3LYP/6-311G and DFT/B3LYP/LanL2DZ, for HCN and Au(CN)x compounds, respectively (no scaling applied).

Each spectrum was jointly fitted and baseline corrected using Voigt profile(s) to fit peaks and a line to adjust for the baseline [23]. The fitting was done in the local area near peaks so that the linear baseline was appropriate. The fitting was carried out using Metropolis–Hastings [13]. Either a mixture of two Voigt profiles or a single Voigt profile was utilized depending on the number of peaks. In the cases where two Voigt profiles were jointly fitted each peak was constrained to be centered ±5 from the desired location. The intensity of each Voigt profile was then used as the intensity response.

3. Results and discussion

3.1. HCN gas experiments

In Fig. 1(c) and (d) the 2133 cm^{-1} vibration is observed in both gas (HCN) and liquid (KCN) SERS experiments. The HCN theoretical vibrational spectrum can explain the origin of the 2133 cm^{-1} mode and corresponds to stretching of C≡N, see insert in Fig. 1(c). In order to understand the origin of experimentally seen vibrations

at 290 and 384 cm^{-1}, additional calculations involving Au-cyanide complexes were performed. We find that Au(CN) and $Au(CN)_2$ display qualitatively similar vibrational spectra, Fig. 1(d). Results show that both 290 and 384 cm^{-1} modes originate from HCN interaction with the Au metal surface, as previously reported by Senapati et al. [26]. This is in accordance with the Elsner equation where the aurat (I) ion complex forms when cyanide is added to gold in the presence of air:

$$4Au + 8CN^- + O_2 + 2H_2O \rightarrow 4[Au(CN)_2]^- + 4OH^-$$

If base is added, cyanide will stay in the CN^- configuration.

In Fig. 2 the SERS spectra of substrates exposed to different flows of 5 ppm HCN(g) are shown. The spectra are recorded 30 min after gas exposure. At lower flows (35; 18; and 9 mL/s) the flow change is reflected in the SERS intensity of the C≡N stretching band at 2133 cm^{-1} (Fig. 2(a)). This indicates that some quantitation is possible at low HCN gas flows. At higher flows (70; 105; 140 and 175 mL/s, Fig. 2(b)) the SERS intensity seems to saturate. Part of the explanation could be that above 35 mL/s most HCN molecules are being "flushed" past the substrate and out of the flow cell, not leaving much time for Au—CN interaction to occur; and therefore only a fraction of the HCN molecules get in actual contact with the SERS substrate. After 4 h the samples were re-measured, and the C≡N stretching band had started to shift +50 wavenumbers. Fig. 3 compares the 35 mL/s gas samples after (a) 30 min, (b) 4 h, and (c) 9 days. It seems as if some dynamics have taken place in favor of the more stable $Au(CN)_2^-$ (aurat (I) ion) complex, in Fig. 3 represented by the extra peak at 2186 cm^{-1}. In total, four bands occurred, at 2133 cm^{-1} and 2186 cm^{-1}, respectively representing the pure C≡N stretching mode of CN^- and the $Au(CN)_2^-$ complex [6,26], and also the Au-C stretching mode at 384 cm^{-1} and the Au-CN bending mode at 290 cm^{-1} are present [26]. The results in Fig. 3 are much similar to those obtained by Premasiri et al. [20] who measured SERS spectra of 0.25–1 ppm NaCN on an Au sol–gel. They report a +50 cm^{-1} shift of the C—N stretching band from low to high CN concentration. We believe the reason for this shift can be that the higher concentrations of cyanide have had sufficient time for dissociation of the Au, forming the mentioned dimer complex. If they had repeated the measurements later either the shift would have been more pronounced or the cyanide would have evaporated as HCN(g). According to Senapati et al. [26] it took about 60 min for a cyanide ion concentration of 800 ppb to dissociate their Au nanoparticles completely, whereas for 800 ppt it would take 180 min. Therefore, at high concentrations the dimer complex forms at a higher rate. The samples of our study were measured again after 9 days, and now the C≡N stretching peak is completely shifted to the 2186 cm^{-1} mode (Fig. 4). It seems as if there is a preference towards the more stable $Au(CN)_2^-$ complex, which increases during storage. This again is in accordance with the results obtained by Senapati et al. [26]. At the same time the Au—CN bending mode at 290 cm^{-1} decreases, probably due to a restricted space for this type of movement in the dimer case. It should be mentioned that the reason why the substrate becomes saturated at a relatively low Raman intensity could be that many hot spots are occupied due to pre-leaning of the nanopillars.

3.2. KCN serial dilution

Since it is difficult to precisely control low concentrations of cyanide in the gas phase, aqueous solutions of KCN were prepared to carry out serial dilution experiments, mimicking lower HCN concentrations in a controllable manner and producing quantitative SERS. KCN is a water soluble powder, and since it is the CN part which is interesting to Raman experiments, KCN in solution works as an optimal model system for precise analysis. To test the correlation between CN concentration and CN Raman signal, KCN solutions from 10 nM to 1 mM were prepared.

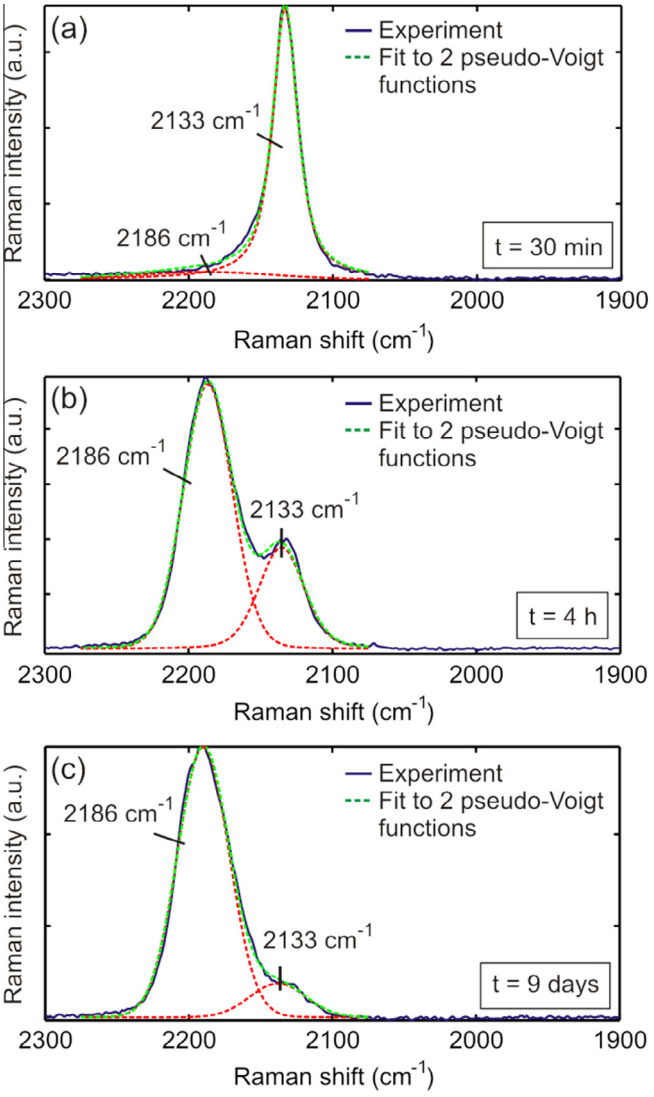

Fig. 3. Representative SERS spectra of 35 mL/s 5 ppm HCN(g) samples measured after 30 min; 4 h; and 9 days. The rearrangement of cyanide from the CN (2133 cm^{-1}) to the $Au(CN)_2^-$ (2186 cm^{-1}) configuration is clearly seen. (Not to scale.)

Representative SERS spectra of the KCN serial solution experiments are presented in Fig. 5(a). The stretching peak of cyanide's triple bond is clear and distinct at ~2137 cm^{-1} where it decreases with decreasing cyanide concentration. As reference, the background spectrum of water (with added NaOH to pH 11) is included for comparison. In Fig. 5(b) the intensity of the stretching peak of C≡N is plotted as a function of KCN concentration. A linear correlation is seen from 100 nM to 1 mM, although it is difficult to distinguish between 100 nM, 10 nM and water. In attempt to distinguish 100 nM from 10 nM KCN and reference samples, principal component analyses (PCAs) including all three cyanide related vibration bands (~2137, 384 and 290 cm^{-1}) were performed, see detailed description in supplementary information. The results indicate that the observed difference between 100 nM and 10 nM KCN concentrations can be largely attributed to signal background fluctuations. However, the results showed nearly a linear relationship between the KCN concentration and the first Principal Component in the 10^{-5}–10^{-7} M KCN concentration range, see Fig. S.6 in supplementary information. This is similar to results

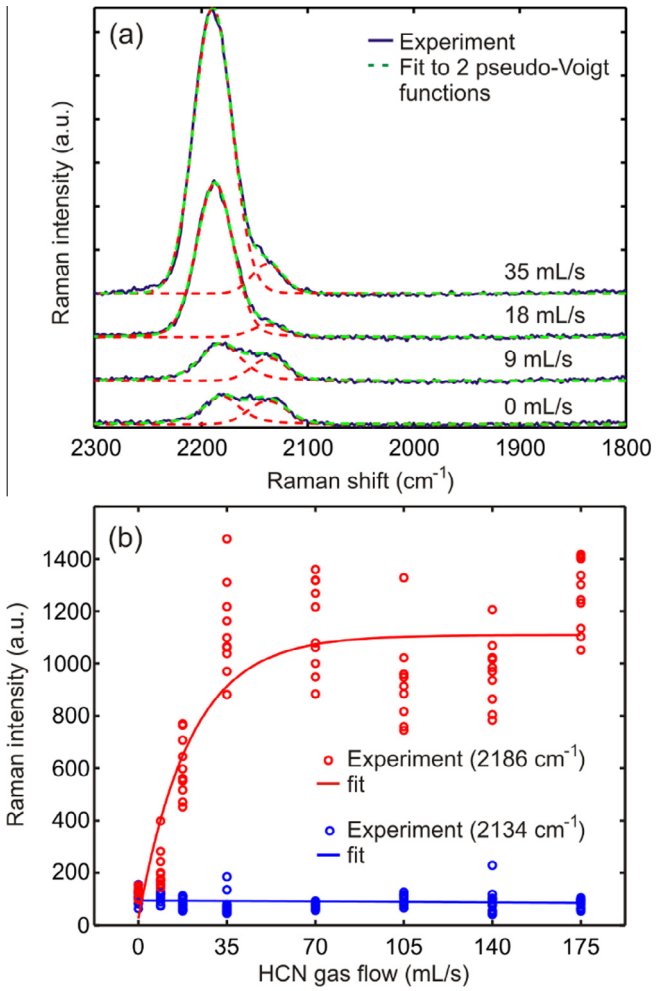

Fig. 4. (a) Representative Raman spectra of the HCN(g) exposed SERS substrates re-measured after 9 days. It is seen that the C≡N stretching mode has shifted to the 2186 cm^{-1} $Au(CN)_2^-$ state. (b) (Blue) 2134 cm^{-1} peak intensity at various gas flows, re-measured after 9 days. There is not much left of the CN monomer. (Red) 2186 cm^{-1} peak intensity at various gas flows, after 9 days. Based on the mean response, Pearson correlation of the intensity of the peaks in Figs. Fig. 2(b) and 4(b) is 0.92. (For interpretation of the references to color in this figure legend, the reader is referred to the web version of this article.)

reported by Thygesen et al. [28] where only the C≡N mode at ~2137 cm^{-1} was utilized in the data analysis. In the latter work, the upper detection limit for a linear relationship between the C≡N band signal intensity and KCN concentration utilizing Au colloids was close to 10^{-5} M while the lower limit was around 10^{-6}–10^{-7} M.

According to Enderby et al. [9] the median value of HCN in the breath of CF children with *P. aeruginosa* lung colonization is 13.5 ppb, which corresponds to 0.75 μM in solution. Explanation is given in the following. Take for instance a 0.05 mL drop of 1 μM KCN weighing approximately 0.05 g. This will contain:

$$0.05\ \mathrm{g}/(18.00\ \mathrm{g/mol}) = 2.8 * 10^{-3}\ mol\ H_2O \text{ and}$$

$$(1 * 10^{-6}\ \mathrm{mol/L}) * (0.05 * 10^{-3}\ \mathrm{L}) = 5.0 * 10^{-11}\ mol\ KCN$$

$$n_{KCN}/n_{H_2O} = (5.0 * 10^{-11})/(2.8 * 10^{-3}) = 18 * 10^{-9} = 18\ ppb.$$

13.5 ppb/18 ppb = 0.75. So, when quantitative SERS applies, the SERS intensity of 0.75 μM cyanide in solution is expected to correspond to the median intensity of the breath of a CF child with PA lung colonization. Breath concentrations for the present application are thus expected to correspond to aqueous cyanide concentrations in the range between 100 nM and 1 μM.

As seen in Fig. 2(b), ~2000 cps seems to be the point of saturation for cyanide in gas phase. The level is similar to 100 μM KCN(aq), which with the above calculations would give 1.8 ppm and not 5 ppm as was the case. This is no surprise as the Au nanopillars used for gas detection were pre-leaned prior to cyanide exposure. Therefore fewer molecules could be "caught" in the hot spots between nanopillars than with cyanide in solution. By letting the alkaline KCN solution dry, all cyanide on the substrate will get in contact with the Au nanopillars, optimizing the Au—CN interaction, including the interaction inside the forming hot spots. It is well-known that pre-leaning of the pillars leads to a lower signal than leaning post-exposure [24]. This means the signal might be expected to be 2–3 times lower with breath than with cyanide in solution; but preliminary tests have shown that the vapor in people's breath is sufficient to make the pillars lean, making pre-leaning unnecessary.

In the serial dilution experiments the C≡N stretching band also shifted during storage, but only when pH had not been adjusted to 11. Like with gas the shift was about 50 cm^{-1} towards higher wavenumbers. Premasiri et al. [20] measured on NaCN(aq) without adjusting the pH. This way Au could dissociate and form the $Au(CN)_2^-$ complex, which probably has led to the shift of the

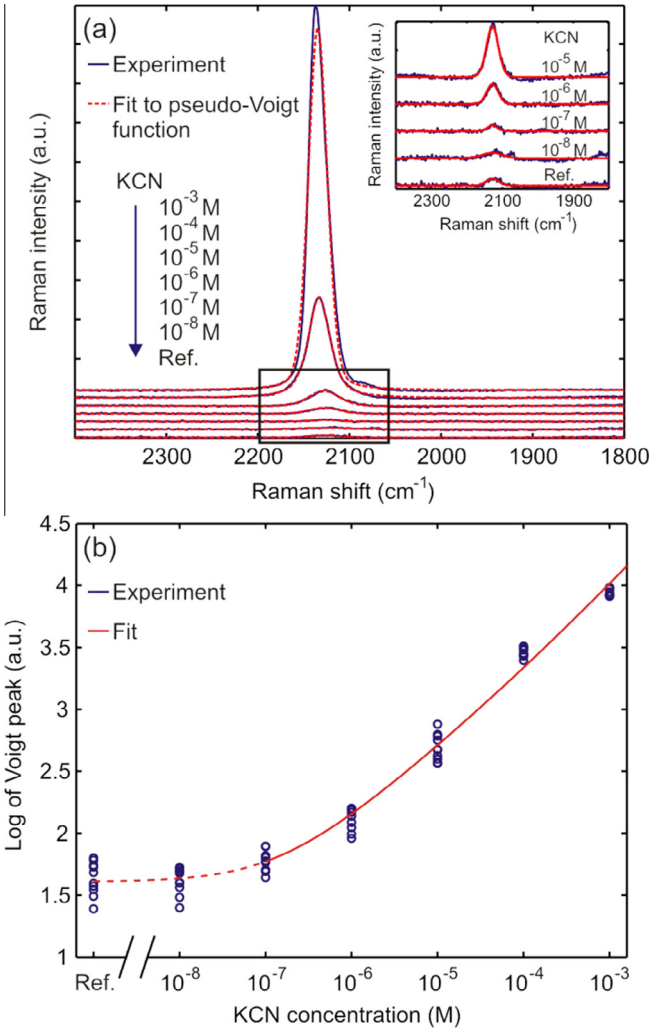

Fig. 5. (a) Representative SERS spectra of KCN concentrations from 10^{-8} to 10^{-3} M and the reference solvent. (b) Raman intensity of the cyanide stretching peak around 2140 cm^{-1} as a function of potassium cyanide concentration. Note log scales on both axes.

C≡N stretching band. When pH is kept high as in the present case, Au will most likely stay as Au^0 and not oxidize to form the aurat (I) ion.

4. Conclusion

By use of the applied SERS technique we have shown that it is possible to quantify the amount of cyanide down to ppb level, which is needed for detection of *P. aeruginosa* lung colonization in the breath of children with cystic fibrosis.

It was possible to distinguish samples with different KCN concentration down to 1 μM (corresponding to 18 ppb) using the C≡N stretching region located close to 2133 cm^{-1}, thus the detection limit was between 18 ppb (detected) and 1.8 ppb (not detected). Future work includes measurements on bacterial cultures and patient samples.

Conflict of interest

The authors declared that there are no known conflicts of interest.

Acknowledgments

The authors would like to thank The Danish Council for Independent Research for supporting the Sapere Aude project "NAPLAS", which this research is part of; Dr. Lotte Bøge Lyndgaard for reviewing the PCA analyses, and PhD stipend Kristian Tølbøl Sørensen for help resolving MATLAB issues. The Novo Nordisk Foundation supported HKJ as a clinical research stipend.

Appendix A. Supplementary data

Supplementary data associated with this article can be found, in the online version, at http://dx.doi.org/10.1016/j.sbsr.2015.07.002.

References

[1] K. Aanaes, L.F. Rickelt, H.K. Johansen, C. von Buchwald, T. Pressler, N. Høiby, P.Ø. Jensen, J. Cyst. Fibros. 10 (2011) 114–120.
[2] L. Bennett, L. Ciaffoni, W. Denzer, G. Hancock, A. Lunn, R. Peverall, S. Praun, G. Ritchie, J. Breath Res. 3 (2009) 046002.
[3] A. Blier, J. Vieillard, E. Gerault, A. Dagorn, T. Varacavoudin, F. Le Derf, N. Orange, M. Feuilloley, O. Lesouhaitier, J. Microbiol. Methods 90 (2012) 20–24.
[4] L.D. Bos, P.J. Sterk, M.J. Schultz, PLoS Pathogens 9 (2013) e1003311.
[5] S.T. Chambers, A. Scott-Thomas, M. Epton, Curr. Opin. Pulmon. Med. 18 (2012) 228–232.
[6] K. Cho, Y.S. Jang, M. Gong, K. Kim, S. Joo, Appl. Spectrosc. 56 (2002) 1147–1151.
[7] J. Dummer, M. Storer, S. Sturney, A. Scott-Thomas, S. Chambers, M. Swanney, M. Epton, J. Breath Res. 7 (2013) 017105.
[8] M. Dyrby, S.B. Engelsen, L. Nørgaard, M. Bruhn, L. Lundsberg-Nielsen, Appl. Spectrosc. 56 (2002) 579–585.
[9] B. Enderby, D. Smith, W. Carroll, W. Lenney, Pediatr. Pulmonol. 44 (2009) 142–147.
[10] F. Gilchrist, R. Bright-Thomas, A. Jones, D. Smith, P. Španěl, A. Webb, W. Lenney, J. Cyst. Fibros. 12 (2013) S83.
[11] J.E. Graham, Adv. Appl. Microbiol. 82 (2012) 29–52.
[12] S.K. Hansen, M.H. Rau, H.K. Johansen, O. Ciofu, L. Jelsbak, L. Yang, A. Folkesson, H.Ø. Jarmer, K. Aanaes, C. von Buchwald, N. Høiby, S. Molin, ISME J. 6 (2012) 31–45.
[13] W.K. Hastings, Biometrika 57 (1) (1970) 97–109.
[14] H.K. Johansen, L. Nørregaard, P.C. Gøtzsche, T. Pressler, C. Koch, N. Høiby, Pediatr. Pulmonol. 37 (2004) 427–432.
[15] H.K. Johansen, K. Aanaes, T. Pressler, K.G. Nielsen, J. Fisker, M. Skov, N. Høiby, C. von Buchwald, J. Cyst. Fibros. 11 (6) (2012) 525–531.
[16] W. Lenney, F. Gilchrist, Eur. Resp. J. 37 (2011) 482–483.
[17] A. Kudelski, B. Pettinger, Chem. Phys. Lett. 321 (2000) 356–362.
[18] J. Ma, P.K. Dasgupta, Environm. Sci. Technol. 44 (2010) 3028–3034.
[19] R.L. Marvig, L.M. Sommer, S. Molin, H.K. Johansen, Nat. Genet. (2014), http://dx.doi.org/10.1038/ng.3148.
[20] W. Premasiri, R. Clarke, S. Londhe, M. Womble, J. Raman Spectrosc. 32 (2001) 919–922.
[21] C.M. Robroeks, J.J. van Berkel, J.W. Dallinga, Q. Jöbsis, L.J. Zimmermann, H.J. Hendriks, M.F. Wouters, Chris P.M. van der Grinten, Kim D.G. van de Kant, F. van Schooten, Pediatr. Res. 68 (2010) 75–80.
[22] B. Ryall, J.C. Davies, R. Wilson, A. Shoemark, H.D. Williams, Eur. Resp. J. 32 (2008) 740–747.
[23] F. Sánchez-Bajo, F.L. Cumbrera, J. Appl. Cryst. 30 (1997) 427–430.
[24] M.S. Schmidt, J. Hübner, A. Boisen, Adv. Mat. 24 (2012) OP11–OP18.
[25] E. Smith, G. Dent, Modern Raman Spectroscopy – A Practical Approach, John Wiley & Sons Ltd, 2005.
[26] D. Senapati, S.S. Dasary, A.K. Singh, T. Senapati, H. Yu, P.C. Ray, Chem. Eur. J. 17 (2011) 8445–8451.
[27] M.D. Stutz, C.L. Gangell, L.J. Berry, L. Garratt, B. Sheil, P. Sly, Eur. Resp. J. 37 (2011) 553–558.
[28] L.G. Thygesen, K. Jørgensen, B.L. Møller, S.B. Engelsen, Appl. Spectr. 58 (2004) 212–217.
[29] T. Wang, A. Pysanenko, K. Dryahina, P. Španěl, D. Smith, J. Breath Res. 2 (2008) 037013.
[30] J. Zhu, H.D. Bean, J. Jiménez-Díaz, J.E. Hill, J. Appl. Physiol. 114 (2013) 1544–1549.
[31] J. Zhu, H.D. Bean, M.J. Wargo, L.W. Leclair, J.E. Hill, J. Breath Res. 7 (2013) 016003.